On the Efficiency of Baroclinic Eddy Heat Transport across Narrow Fronts*

MICHAEL A. SPALL AND DAVID C. CHAPMAN

Department of Physical Oceanography, Woods Hole Oceanographic Institution, Woods Hole, Massachusetts

(Manuscript received 12 August 1997, in final form 2 February 1998)

ABSTRACT

A simple theory is developed that relates the amplitude of eddy heat (or density) flux across a narrow front to the basic frontal parameters. By assuming that heat is transported primarily by baroclinic eddy pairs, an analytical expression for the cross-front eddy heat flux is derived as

$$\overline{u'\rho'} = c_e V_m \Delta\rho,$$

where u' and ρ' are deviations from the temporal or spatial mean cross-front velocity and density, $\Delta\rho$ is the density change across the front, V_m is a scale for the alongfront velocity (which may be interpreted as the maximum alongfront velocity for a front with density change $\Delta\rho$ over a horizontal scale of the deformation radius, assuming a deep level of no motion), and c_e is an efficiency constant. Similar expressions for the eddy heat flux have been proposed previously, based on scaling or energetics arguments, but neither an a priori estimate for the value of the efficiency constant c_e nor a clear dynamical understanding of what determines its value has been forthcoming. The theory presented here provides a dynamically based means of estimating the efficiency constant, which may be approximately interpreted as the ratio of the speed at which eddies propagate away from the front to the alongfront velocity, resulting in $c_e \approx 0.045$. Eddy-resolving numerical models are used to test this theoretical estimate for both unforced and forced frontal problems. For a wide range of parameters the cross-frontal heat transport is carried primarily by heton-like eddy pairs with values of c_e between 0.02 and 0.04, in general agreement with the theory. These values of c_e are also consistent with numerous previously published laboratory and numerical studies.

1. Introduction

An understanding of how eddies transport tracers is of intrinsic importance because eddies constitute a fundamental component of the general oceanic and atmospheric circulations. There has been much recent work related to parameterizing the transport of passive and active tracers by mesoscale eddies (e.g., Gent and McWilliams 1990; Larichev and Held 1995; Visbeck et al. 1996, 1997; Treguier et al. 1997), which has been at least partially motivated by the desire to represent small-scale processes in large-scale climate models without the need to explicitly resolve the variability on mesoscale time and space scales. It is well known that the eddy field in the ocean is spatially nonhomogeneous, with increased eddy variability generally found in the vicinity of strong lateral density gradients, that is, narrow fronts (Treguier et al. 1997). This correspondence has led to the development of parameterizations of the eddy fluxes in terms of the local properties of the large-scale flow (Green 1970; Stone 1972; Gent and McWilliams 1990; Treguier et al. 1997; Visbeck et al. 1997). These parameterizations vary considerably in their details (e.g., isopycnal vs diapycnal, see Visbeck et al. 1997), but they typically represent the eddy fluxes as a diffusion down the mean property gradient. Green (1970) (see also Stone 1972) used energetics arguments to suggest that the magnitude of the horizontal eddy diffusivity K is proportional to a length scale squared and inversely proportional to the Eady timescale for exponential growth,

$$K = c_e f L^2/\sqrt{\mathrm{Ri}}, \tag{1}$$

where f is the Coriolis parameter, L is the length scale of the large-scale baroclinic flow, and $\mathrm{Ri} = N^2/V_z^2$ is the Richardson number of the large-scale flow with buoyancy frequency given by N and vertical shear of the alongfront velocity given by V_z. The nondimensional scale factor c_e, which we call the efficiency constant to avoid possible confusion with the various definitions of similar proportionality constants that have previously appeared in the literature, is unknown and presumed by Green (1970) to be constant. This proportionality con-

* Contribution Number 9485 from Woods Hole Oceanographic Institution.

Corresponding author address: Dr. Michael A. Spall, Department of Physical Oceanography, Woods Hole Oceanographic Institution, MS#21, Woods Hole, MA 02543.
E-mail: mspall@whoi.edu, dchapman@whoi.edu

stant can be thought of as a correlation coefficient between the swirl velocity of the eddies and the density anomaly, typically much less than 1.

If the lateral eddy heat flux is assumed proportional to the product of the diffusivity and the large-scale density gradient, then, using the thermal wind relation, the eddy heat flux can be written as

$$\overline{u'\rho'} = K\partial\rho/\partial x = c_e V_m \Delta\rho, \qquad (2)$$

where u' and ρ' are deviations from the large-scale time and/or spatial average mean quantities, $\Delta\rho$ is the cross-front change in density over a horizontal length scale L, and V_m is a scale for the alongfront velocity, which may be interpreted as the maximum alongfront velocity for a front with density change $\Delta\rho$ over a horizontal scale of the deformation radius (assuming a deep level of no motion).[1] Note that (2) is independent of the length scale L, and that the eddy heat flux $\overline{u'\rho'}$ is in the x direction, perpendicular to the mean flow V (the direction of the mean flow is assumed here to be uniform with depth).

Several recent studies have made use of this formalism to parameterize the lateral heat transport by baroclinic eddies (e.g., Visbeck et al. 1996, 1997; Legg et al. 1996; Chapman and Gawarkiewicz 1997; Jones and Marshall 1997). Configurations in which buoyancy is extracted from the surface of an initially resting ocean develop strong baroclinic rim currents that are very nearly in geostrophic balance with the density gradient that develops around the edge of the cooling region. For forcing regions large compared to the deformation radius, the rim currents are baroclinically unstable and shed eddies, leading to a quasi-equilibration between the lateral (and vertical) heat transport carried by the eddies and the heat loss to the atmosphere. The properties of the cooling region (depth and density) have been predicted by applying the eddy heat flux parameterization proposed by Green (1970). The efficiency constant c_e, an unknown in the problem, has been estimated by empirical fit to the data. Visbeck et al. (1996) found that $c_e \approx 0.025$ (with variability between 0.014 and 0.056) over a wide range of forcing parameters in both numerical and laboratory experiments.[2] Applications of similar ideas to shallow convection in coastal regions (Chapman and Gawarkiewicz 1997; Chapman 1998), unforced baroclinic frontal zones, and wind-forced periodic channels (Visbeck et al. 1997) all produce similar values of c_e. These results suggest that the formulation proposed in (2) is valid (at least for the problems tested) and that the efficiency constant c_e is independent of all external parameters. While this form is dimensionally consistent, there is no reason a priori that c_e should be independent of external parameters (such as the Burger number or the Richardson number), nor has there been a physical justification for the nearly constant value of c_e.

The purpose of this study is to derive a quantitative estimate of the eddy heat flux in frontal zones and to provide a physical interpretation of what controls the magnitude of the heat flux and its dependencies on the basic frontal parameters. For simplicity, we restrict our attention to narrow fronts, that is, those whose cross-front length scale is of the order of the internal deformation radius. We show that an estimate of the heat flux derived explicitly from a model of eddy interactions and heat transport results in a form similar to that proposed by Green (1970). Perhaps the most important result of this study is that the simple model used to estimate the magnitude and dependencies of the eddy heat flux also provides a physically based means to calculate the efficiency constant c_e. The theoretical estimate is tested by comparison with eddy-resolving models in two different flow configurations.

2. Isopycnal heat transport by baroclinic eddies

Our goal is to estimate the isopycnal eddy heat flux across a baroclinic front. Diapycnal mixing could also be added, but we view this as a separate process from the isopycnal transport carried by coherent vortices, as discussed by Gent and McWilliams (1990) and Visbeck et al. (1997). The eddy heat flux $\overline{u'\rho'}$ could, in principle, be calculated directly as the space and/or time average of the product of the perturbation velocity and the perturbation density. However, it is difficult to estimate $\overline{u'\rho'}$ a priori because it involves an unknown correlation between the two quantities that is typically much less than one. Furthermore, a variety of complicated dynamical mechanisms may contribute to the time-dependent and spatially varying motions, including propagation of coherent vortex structures, nonlinear waves and wave breaking, and small-scale turbulence and mixing. Nevertheless, considerable progress can be made if we assert from the outset that the dominant mechanism of eddy heat transport across baroclinically unstable fronts is through the formation and propagation of individual eddies with length scale on the order of the internal deformation radius. This is consistent with the previous studies mentioned in the introduction, and it allows the relatively simple interpretation that the heat flux carried by each eddy is the product of the average density anomaly of the eddy and its propagation speed away from the front.

We are interested only in the eddy heat flux across

[1] Strictly speaking, (2) defines an eddy density flux, not an eddy heat flux. However, for simplicity, we assume the density is linearly proportional to the temperature and independent of salinity. Thus, (2) is equivalent to an eddy heat flux.

[2] Visbeck et al. (1996) used a velocity scale in their scaling arguments for deep convection that is three times the actual estimated vertical change in geostrophic velocity associated with the rim current [see Jones and Marshall's (1997) Eq. (2.4)]. Therefore, c_e used here in (2) is three times the α' defined by Visbeck et al. (1996).

the front, so we assume that all eddies are formed at the front, move away and never return. This is approximately true in the model calculations, although some eddies do eventually return to the frontal zone after formation. We do not try to parameterize their ultimate decay and disappearance. In keeping with this perspective, we limit the analysis to narrow fronts, that is, those whose cross-front length scale is approximately the internal deformation radius ($L \approx L_d$). This view is also motivated by previous laboratory and numerical modeling studies, and the observation that the largest eddy activity in the ocean is found in the vicinity of narrow fronts. Furthermore, we expect that wider fronts may introduce additional complications because another length scale is introduced into the problem and the properties of the eddies (i.e., density, propagation speed) will depend on their origin and mixing along their path.

Spatial and temporal averaging of the heat flux carried by eddies will necessarily be reduced compared with that carried by an individual eddy. Spatial averaging along the front over a wavelength immediately reduces the heat flux by one half. Temporal averaging is more difficult to quantify. Eddy shedding typically occurs quasiperiodically with some time required for the front to develop large amplitude meanders between eddy shedding events. The theory developed here is appropriate for the large amplitude meandering regime. The fraction by which the eddy heat flux will be reduced due to temporal averaging can be approximated by

$$\frac{1}{1 + \tau_l/\tau_{nl}}, \tag{3}$$

where τ_l is a linear growth timescale and τ_{nl} is a nonlinear timescale, which we interpret as the time it takes eddies to form and propagate away from the front. While it is difficult to define these timescales precisely, the numerical calculations in section 3 (Fig. 4a, for example) can be used to obtain a rough estimate of (3), suggesting a modest reduction in the eddy flux of $O(35\%)$. However, because these estimates are difficult to quantify a priori, and because we are primarily interested in gaining a simple phenomenological understanding of what controls the amplitude of the eddy heat flux, we do not attempt to formally incorporate this effect in our estimate of c_e. Our estimate should thus be viewed as an upper bound in this regard.

The large space- and timescale average eddy heat flux may now be written

$$\overline{u'\rho'} = \frac{1}{2}u_e\rho_e, \tag{4}$$

where u_e is the propagation speed of an eddy away from the front, and ρ_e is the density anomaly of the eddy relative to the mean stratification of the motionless ocean on one side of the front. The primary advantage of this formulation is that it implicitly removes the need to know the correlation between the eddy swirl velocity and the density anomaly. For narrow frontal regions the density anomaly of the eddies will be either $\Delta\rho$ or zero, depending on which side of the front they originate. If density is conserved following the Lagrangian path of an eddy, the density anomaly of that eddy does not change in time (as we have defined it here), although its density anomaly relative to the ambient fluid may change.

Combining (2) and (4), the efficiency constant c_e may now be written in terms of the eddy propagation speed as

$$c_e = \frac{u_e}{2V_m}. \tag{5}$$

The task is now to determine u_e. In order for (2) to be valid, c_e must be independent of all frontal parameters; that is, $u_e = u_e(V_m)$.

We consider a large-scale flow that is uniform in the alongfront direction. Variations in both bottom topography and planetary vorticity are ignored. The most likely mechanism by which baroclinic eddies transport heat along isopycnals in such a flow is by eddy–eddy interactions, or self propagating eddy pairs. Hogg and Stommel (1985) first noted the rapid and efficient heat transport resulting from the pairing of upper-layer and lower-layer eddies of opposite sign, which they called hetons. Pedlosky (1985) found this structure to be the preferred orientation of the fastest growing mode based on a linear stability analysis of strong frontal regions. Legg et al. (1996) demonstrated that the heton model provides a useful approximation for the spread of heat away from a cooling region by baroclinic eddies. Therefore, we make use of the heton mechanism to estimate u_e.

For simplicity, we assume that the frontal region and surrounding ocean are represented by two layers of different density with a reduced gravity $g' = g(\rho_2 - \rho_1)/\rho_0$, where ρ_0 is a reference density for seawater (Fig. 1a). For narrow fronts of width $L_d = \sqrt{g'H}/f$, the maximum alongfront velocity (assuming no motion in the deep layer) is $V_m = \sqrt{g'h}\sqrt{h/H}$, where H is a scale height for the mean stratification and h is the vertical displacement of the interface across the front.

It is assumed that the eddies are quasigeostrophic so that the perturbation of the interface in the eddies is small compared to the resting layer thickness. This assumption is clearly not satisfied in some of the previous numerical and laboratory experiments where the density surfaces outcrop, but we make this assumption here in order to obtain a quasi-analytic solution. The large amplitude regime is investigated numerically in section 3. We assume that the eddies represent isolated volumes of water that originated from the other side of the front and have been transported across the front by large-amplitude baroclinic wave events and resulting ageostrophic cross-front velocities accompanying baroclinic instability (Spall 1995), a reasonable assumption for fronts of width L_d. In this case, the eddies have uniform potential vorticity dictated by the thickness of each layer

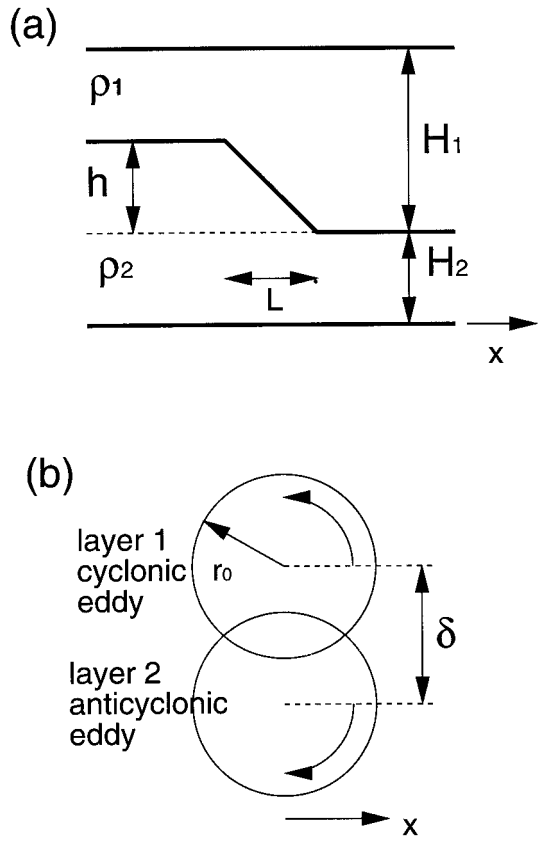

FIG. 1. Schematic diagrams of (a) vertical section through the baroclinc front and (b) plan view of a heton eddy pair.

on the original side of the front. Thus, the thickness anomaly of the eddies will be of different sign in the upper and lower layers, giving rise to one cyclonic vortex and one anticyclonic vortex [see Pedlosky (1985) and Spall (1995) for a discussion on the formation of hetons from baroclinic fronts]. We assume that the eddies are axisymmetric with radius r_0 and that their structure is unaffected by the presence of the eddy in the other layer. Stronger eddies tend to be more elliptical but have only slightly slower propagation speeds (Polvani 1991).

The self-propagation speed of baroclinic eddy pairs driven by the interaction between upper- and lower-layer eddies in a quasigeostrophic ocean on an f plane may be written as (Pakyari and Nycander 1996)

$$u_e = \frac{\int xJ(\psi_1, \psi_2)\, dA}{\int (\psi_1 - \psi_2)\, dA}, \tag{6}$$

where x is the distance perpendicular to the front, ψ_n is the quasigeostrophic streamfunction in layer n, and $J(\psi_1, \psi_2) = (\partial\psi_1/\partial x)(\partial\psi_2/\partial y) - (\partial\psi_2/\partial x)(\partial\psi_1/\partial y)$ is the Jacobian operator. The integrals are taken over the horizontal area A, assumed to encompass the entire eddy pair. As shown by Pakyari and Nycander (1996), the propagation speed is a function of the horizontal distance between the eddy centers, that is, the offset δ (see Fig. 1b). If there is no offset and the upper-layer eddy is of the same structure and opposite in sign to the lower-layer eddy, the Jacobian vanishes and there is no self-propagation. If the offset is small, Pakyari and Nycander state that the propagation speed increases linearly with δ/r_0 and with the eddy swirl velocity. For eddies of finite radius, in which the velocity goes to zero outside of the radius r_0, we anticipate that the eddy–eddy interaction will decrease at large δ because the area over which the eddies overlap will decrease; $J(\psi_1, \psi_2) \to 0$ [the denominator in (6) does not depend on the offset].

An approximate closed form solution for u_e, and hence the resulting eddy heat flux and c_e, can be obtained if we assume that the relative vorticity is uniform within each eddy and that the decrease in propagation speed as the offset increases arises solely as a result of the decreasing area of interaction between the eddies. An approximate solution may be derived from the small offset limit, for which, following Pakyari and Nycander (1996), (6) can be written in terms of the lateral offset δ, the swirl velocity in each layer v_n, and the quasigeostrophic streamfunction as

$$u_e = \frac{\delta \int v_1 v_2\, dA}{2\int (\psi_1 - \psi_2)\, dA}. \tag{7}$$

For quasigeostrophic, uniform relative vorticity eddies, the velocity profile is linear with radius, $v(r) = v_m r/r_0$, where v_m is the maximum swirl velocity of the eddy. The quasigeostrophic streamfunction for each eddy is then quadratic with radius,

$$\psi_n = (-1)^{n+1}(g'h/f)(1 - r^2/r_0^2),$$

where h is the thickness anomaly at the center of the eddy [assumed here to be the same as the interface displacement across the front, this approximation is valid for $B = (L_d/r_0)^2 \ll 1$, Spall (1995)]. Substituting for the velocity and streamfunction, (7) may be written as

$$u_e = \frac{\delta f v_m^2 \int r^2\, dA}{4g'h\int (r_0^2 - r^2)\, dA}. \tag{8}$$

The eddies are presumed to have been generated through baroclinic instability of the frontal zone, so the eddy radius is taken to be a function of the deformation radius, $r_0 = 2\sqrt{2}L_d$ (see Killworth 1983 and Spall 1995 for similar discussions). This gives a Burger number for the eddies of $B = 0.125$ [direct numerical integrations

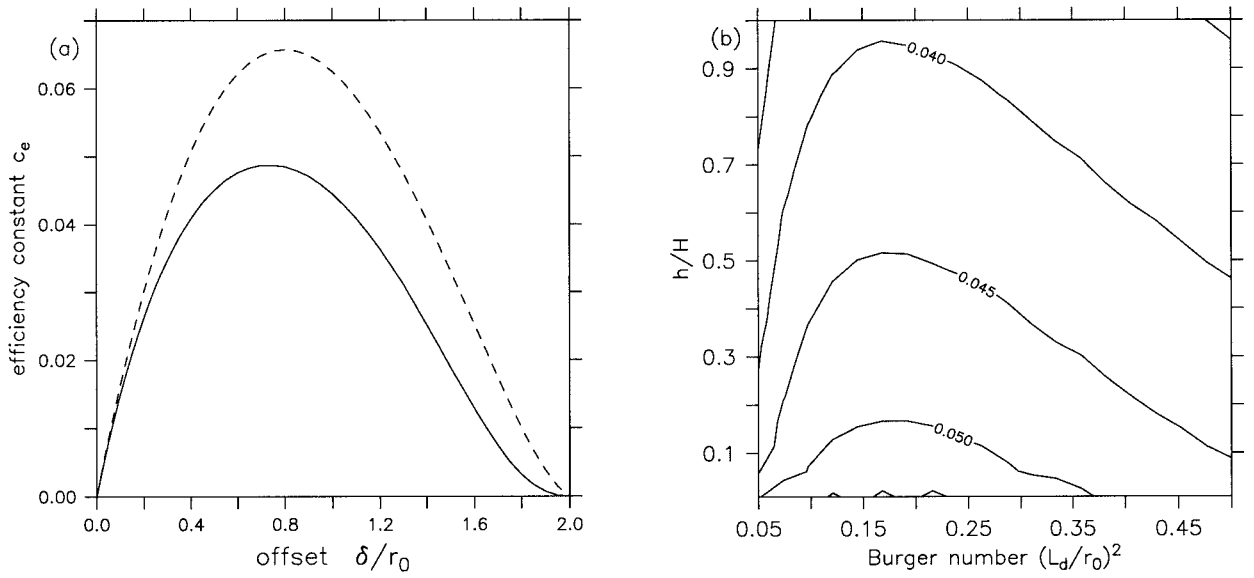

FIG. 2. (a) Efficiency constant c_e as a function of vortex offset δ/r_0. Solid line: formal estimate from (5) and (6) for uniform potential vorticity eddies. Dashed line: approximate closed form solution (12). (b) Efficiency constant c_e as a function of Burger number $B = (L_d/r_0)^2$ and interface displacement h/H from (5) and (6), assuming $\delta/r_0 = 1$.

of (6) show that c_e is only weakly dependent on B, as shown below]. The maximum swirl velocity is obtained from $v = \psi_r$ evaluated at $r = r_0$, resulting in $v_m = 2\sqrt{g'h^2B/H} = 2\sqrt{B}V_m$. The propagation speed of the eddy, in the small offset limit, is estimated by integrating (8) to give

$$u_e = \frac{\sqrt{2}}{4}\frac{\delta}{r_0}\sqrt{g'h}\sqrt{h/H} = \frac{\sqrt{2}}{4}\frac{\delta}{r_0}V_m. \qquad (9)$$

For large offsets, we assume that the propagation speed of the eddy pair decreases in proportion to the decreasing area of overlap. Using a truncated series approximation to estimate the area of overlap, the propagation speed u_e for large offsets is then estimated to be

$$u_e \approx \frac{\sqrt{2}}{4}\frac{\delta}{r_0}(1 - \delta/2r_0)^{3/2}V_m, \qquad (10)$$

and the eddy heat flux becomes

$$\overline{u'\rho'} \approx \frac{\sqrt{2}}{8}\frac{\delta}{r_0}(1 - \delta/2r_0)^{3/2}V_m\Delta\rho. \qquad (11)$$

While this solution is not a formal limit of the integral relation (6), it does indicate several important properties of the way in which the eddy pairs transport heat. First, (11) supports the assertion of Green (1970) that the eddy heat flux is linearly related to the product of the density change across the front and the alongfront velocity. The eddy flux is reduced for weak frontal zones because the propagation speed of the heton pair depends on the change in interface thickness over the eddy radius (h), while the size of the eddies is related to the mean stratification H through the deformation radius. For $h \ll H$ the eddies propagate more slowly than similar sized eddies with $h = O(H)$ (see definition of V_m). For the convection problems discussed by Visbeck et al. (1996), Jones and Marshall (1997), Chapman and Gawarkiewicz (1997), and Chapman (1998), the interface displacement h is the same as the resting depth of the interface H because the interface outcrops. Equation (11) also demonstrates that the eddy heat flux increases with increasing density change across the front by two mechanisms: the eddies have a larger density anomaly relative to the surrounding water and their propagation speed increases as $\Delta\rho^{1/2}$ through V_m.

Combining (11) with (2) provides a quantitative estimate of the efficiency constant c_e,

$$c_e \approx \frac{\sqrt{2}}{8}\frac{\delta}{r_0}(1 - \delta/2r_0)^{3/2}, \qquad (12)$$

which indicates that the efficiency constant c_e is independent of all external parameters and depends only on the relative offset of the upper- and lower-layer eddies. Thus, the efficiency of the eddy heat flux across a narrow frontal region is essentially determined by the ratio of the propagation speed of the eddies to the alongfront velocity.

The value of c_e from (12) is shown in Fig. 2 by the dashed line. For small vortex offsets ($\delta/r_0 \ll 2$), c_e increases linearly with δ/r_0, as suggested by Pakyari and Nycander (1996). As δ/r_0 increases, the area of interaction decreases and the vortex propagation speed decreases, eventually vanishing as $\delta/r_0 \to 2$ (the finite radius eddies no longer interact when $\delta/r_0 > 2$). The maximum value of c_e can be calculated directly from (12) as $c_e = 0.064$, which occurs at an offset of $\delta/r_0 = 0.8$.

A more accurate estimate of the eddy propagation speed, and hence the efficiency constant c_e, can be obtained directly from (6) using the streamfunction derived from the uniform potential vorticity solutions given in Spall (1995). The parameters required to fully define the eddy structure, and ψ_n in (6), are the layer thicknesses on both sides of the front and the Burger number $B = (L_d/r_0)^2$. For purposes of comparing the integral solution with the approximate solution for c_e we initially take $B = 0.125$, $h = 0.5H$ with $H_1 = H_2 = H$. The streamfunction is assumed to be constant (zero horizontal velocity) outside of the maximum radius of the eddies.

The value of c_e estimated directly from (5) and (6) is shown by the solid line in Fig. 2a as a function of the lateral offset between vortex centers δ/r_0. The integral solution compares reasonably well with the approximate closed form solution (12), confirming that the primary cause of the decrease in propagation speed for increasing offsets is the decreasing area of overlap between the eddies. Point vortex models will thus overestimate the efficiency of the lateral heat transport by finite radius heton pairs. This may partially explain the larger value of c_e found by Legg et al. (1996) for heat transport carried by point vortex hetons when compared to high-resolution numerical simulations. The maximum propagation speed occurs for offsets close to the radius of the eddies ($\delta/r_0 \approx 1$).

In general, the vortex offset δ/r_0 remains an unknown parameter. The linear stability analysis of Pedlosky (1985) provides a physically based means of estimating the offset expected in the vicinity of the frontal region. His analysis shows that the maximum growth rate occurs for a heton pair with an offset of $\delta/r_0 \approx 1$, close to the offset that produced the maximum propagation speed for the isolated vortex pair found above (Fig. 2). This value may be interpreted as a phase shift between the upper layer and the lower layer of 90°, as expected for baroclinically unstable waves. We assume here that the offset in our frontal eddies is determined by the behavior of the linearly most unstable mode as derived by Pedlosky (1985) and take $\delta/r_0 = 1$. We note that c_e is not strongly dependent on our choice of δ/r_0 in that $c_e > 0.04$ for $0.4 < \delta/r_0 < 1.1$.

The approximate solution suggests that the value of c_e, as defined in (2), is independent of all other parameters. This need not be so, however, as additional nondimensional factors involving h/H or B might be involved. The value of c_e calculated from (5) and (6) with $\delta/r_0 = 1$ is shown in Fig. 2b as a function of the interface displacement across the front h/H and the Burger number of the eddies. The value of c_e is nearly constant for wide ranges of both the eddy radius and the interface displacement, reinforcing the functional relationship suggested by the approximate solution (11). We take as our estimate for the efficiency constant the average over all values of h/H at $B = 0.125$, resulting in $c_e = 0.045$ (averaging over all values of B gives $c_e = 0.043$).

Our estimate of c_e is essentially independent of all model parameters; the only provision is that rotation is important to the dynamics. This implies that the heat flux carried by the eddies does not depend on how the frontal region is maintained, provided that the front is baroclinically unstable. It should be kept in mind, however, that many simplifying assumptions have been made in obtaining this estimate, so we present numerical calculations in the next section to provide support for the theory.

3. Numerical model results

High-resolution numerical models are now used to evaluate (2) for the lateral heat transport by baroclinic eddies. The purpose of these calculations is twofold: 1) to confirm that the dominant mode of lateral heat transport is characterized by baroclinic dipole pairs (hetons) and 2) to quantify the rate at which these eddy pairs transport heat perpendicular to the front. Although similar calculations have already been reported in the literature (as summarized in the introduction and also below), we briefly present two sets of calculations in which the efficiency of the eddy heat fluxes is calculated in a manner consistent with the definition (2) for both weak and strong fronts. This allows for a quantitative evaluation of the theoretical estimate of the eddy heat transport, and also demonstrates the applicability of this idealized model of eddy heat transport to a range of situations.

a. Spindown of an unforced front

The first application is that of the spindown of an initially narrow frontal region in the absense of any external forcing (as in Spall 1995). Small perturbations initialized along the frontal region grow in time, eventually reaching sufficient amplitude to form separated vortices that can transport heat across the front. Spall (1995) noted that the eddies can pair up with eddies in the opposite layer to form baroclinic dipole pairs that transport heat away from the frontal region. The structure of these eddy pairs is in general agreement with the heton model of Hogg and Stommel (1985) and the linear stability theory of Pedlosky (1985). Calculations similar to those reported here have also been analyzed by Visbeck et al. (1997); however we extend the analysis into the small h/H limit not investigated in the previous convection problems.

Only a brief review of the model is given here; for a more complete description the reader is referred to Spall (1995) and the references therein. The model solves the primitive equations of motion in isopycnal coordinates. Calculations are carried out with both two and three layers in the vertical with a reduced gravity between each of the layers of 0.003 m s^{-2}. The domain is 500 km $\times$ 500 km square with horizontal grid spacing of 2 km (251 $\times$ 251 grid points). The Coriolis parameter

$f = 10^{-4}$ s^{-1} and is constant. The stratification is such that each of the layers is $H_n = H = 400$ m thick on the anticyclonic side of the front. The interface between layers 1 and 2 is displaced by an amount h over a horizontal scale of $L = L_d = \sqrt{g'H}/f = 10$ km such that the thickness of layer 2 (1) is greater (less) on the cyclonic side of the front than it is on the anticyclonic side of the front. For the cases with three layers, the interface between layers 2 and 3 is initially flat. The reference level is chosen so that there is initially no flow in the deepest layer. Mass exchange is not allowed between layers. Subgrid-scale mixing is parameterized by a Laplacian thickness diffusion with amplitude 10 m^2 s^{-1}. The frontal region is initialized with small perturbations of wavelengths between 25 and 250 km. From these initial conditions the model is integrated for at least $500\sqrt{\text{Ri}}/f$, where $\sqrt{\text{Ri}}$ can be written as H/h.

The horizontal velocity together with the potential vorticity for layers 1 and 2 on day 14 are shown in Figs. 3a and 3b. This calculation has only two layers and was initialized with $h = 100$ m, or 25% of the resting layer thickness. The structure of the growing meanders is essentially the same as predicted by the linear theory of Pedlosky (1985), and whose large amplitude development is described in detail by Spall (1995). On the anticyclonic (warm) side of the front, troughs of cyclonic (high) potential vorticity extend away from the initial frontal position. In the second layer, there are deep anticyclonic vortices of low potential vorticity adjacent to the upper-layer cyclones. The deep anticyclones are positioned just upstream of the cyclones with an offset $\delta/r_0 \approx 1$, consistent with the most unstable mode predicted by Pedlosky (1985). This hetonic structure is self-propagating so that these density anomalies are advected away from the frontal region. Similar structures are found for all values of h tested. These results confirm that for the flat-bottom, f-plane cases studied here the heat transport is carried primarily by baroclinic eddy pairs.

The efficiency constant c_e can be estimated directly from the model fields by making use of (2),

$$c_e = \frac{\overline{u_1'h_1'} + \overline{u_2'h_2'}}{V_m h}, \tag{13}$$

where $\overline{u_n'h_n'}$ is the alongfront average of the eddy thickness flux perpendicular to the front for layer n.

The value of c_e fluctuates in time as individual cycles of meander growth and vortex formations take place. This is illustrated in Fig. 4a by a typical time series of the efficiency constant c_e calculated at the middle of the channel using (13). As expected, the value of c_e is small early in the calculation because the initial meanders take some time to form. The eddy flux peaks as the baroclinic waves reach large amplitude, producing a maximum value of approximately 0.05 at about day 37. This peak value is similar to, but slightly larger than, the theoretical value of 0.045 derived in the previous section. The amplitude of the eddy heat flux then fluctuates as cycles of eddy growth and propagation away from the front continue. Eventually, the calculated c_e decreases over a longer-time scale because the potential energy of the front is reduced as a result of the eddy heat flux and a narrow front no longer exists. This late stage appears more turbulent than the early fields in Fig. 3, however the eddies still propagate through the formation of heton-like pairs.

An objective measure of the amplitude of c_e in the narrow-front regime is obtained by taking the maximum of a running average over a time period $\tau = 200\sqrt{\text{Ri}}/f$. For reference, the Eady linear growth timescale based on a channel width of $2L_d$ is approximately $6\sqrt{\text{Ri}}/f$. This approach smooths the high-frequency variations in the eddy flux associated with individual instability cycles and thus gives a value representative of the average eddy heat flux. The running average is indicated by the dashed line in Fig. 4a and has a maximum value of $c_e = 0.031$. While different averaging procedures produce slightly different estimates of c_e, all methods tested give similar results.

While our primary objective is to estimate the eddy heat flux in (2), the intermediate relations relating the eddy flux to the eddy propagation speed, (4) and (5), can also be tested. The propagation speed of an eddy pair for a case with an outcropping front was calculated by Spall (1995) to be $u_e = 3.5$ cm s^{-1}. With the model parameters $h = 100$ m and $g' = 0.003$ m s^{-2}, $V_m = \sqrt{g'h} = 55$ cm s^{-1}, resulting in $c_e = 0.032$, very close to the values estimated from a direct calculation of the eddy heat flux in (13). It is difficult to apply this estimate in a general sense to the fully evolving frontal region, particularly in the large amplitude turbulent regime, because of the difficulties with identifying and tracking individual eddies in the vicinity of the front.

A series of spindown front calculations using both two and three layers have been carried out in which the initial thickness change across the front has been varied from $h = 0.125H$ to $h = H$ (outcropping front). The maximum value of c_e taken from the running time mean over a time period $\tau = 200\sqrt{\text{Ri}}/f$ is shown in Fig. 4b as a function of the thickness change across the front h/H. The efficiency constant c_e for both two and three layers varies between 0.030 and 0.046 over all ranges of the frontal strength. The average value of c_e taken from all of the two layer calculations is 0.035, within 35% of the theoretical estimate of 0.045 and similar to the value found by Visbeck et al. (1996, 1997) of 0.025. The average for the three layer calculations is 0.036.

Additional calculations have been made in which the Coriolis parameter was reduced or increased by a factor of 2 and they resulted in similar values of c_e, ranging between 0.025 and 0.039. Introducing a cross-front gradient in f of magnitude $\beta = 2 \times 10^{-13}$ cm^{-1} s^{-1} gave essentially identical results to the f-plane results shown here.

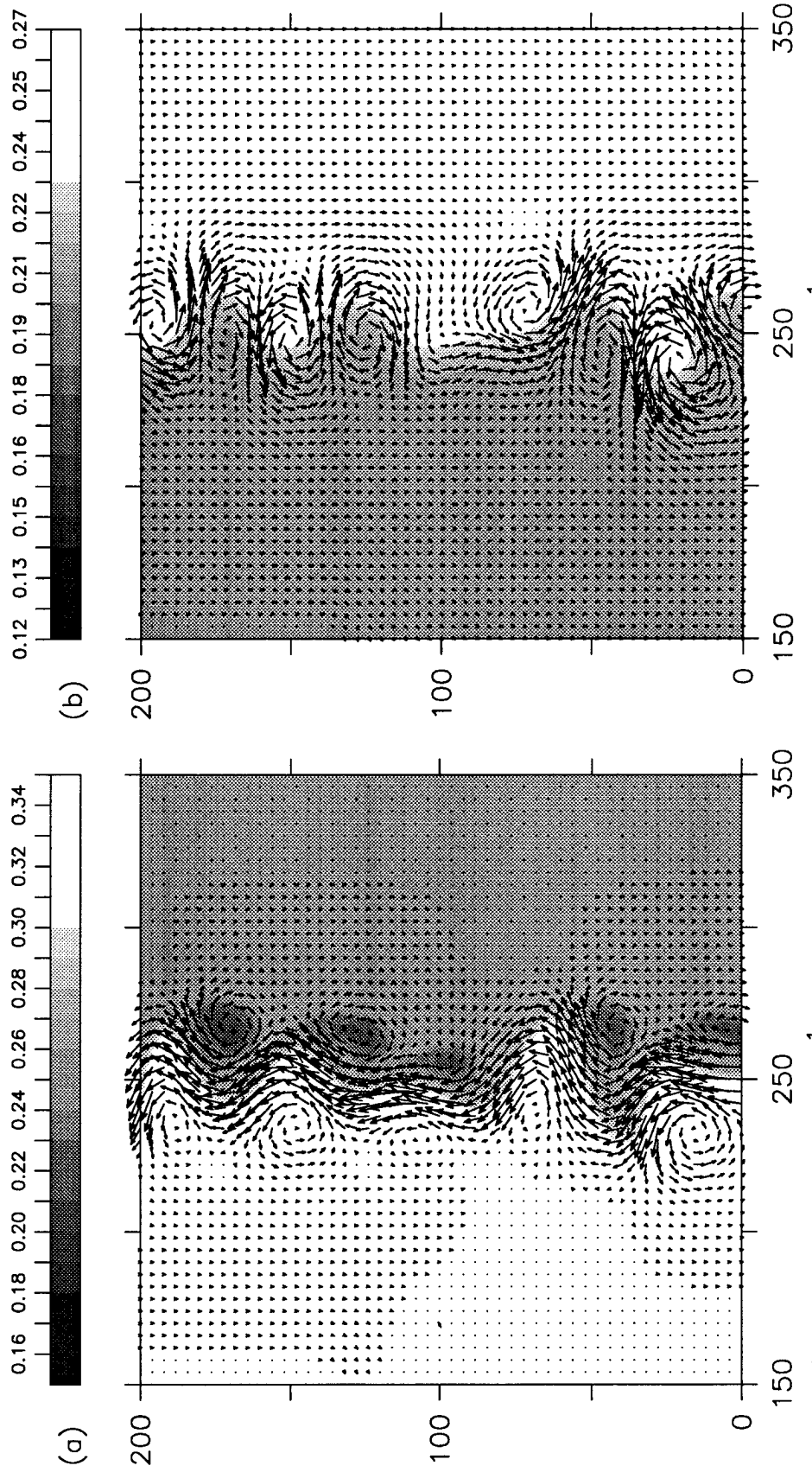

FIG. 3. Horizontal velocity (plotted every other grid point) and potential vorticity on day 14 over a subregion of the model domain for the two layer spindown front problem with $h/H = 0.25$: (a) layer 1 and (b) layer 2.

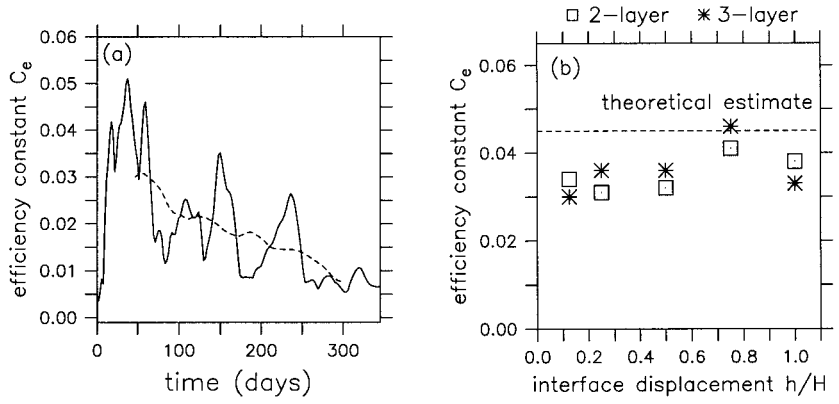

FIG. 4. (a) Time series of the efficiency constant c_e for the two layer case with $h/H = 0.25$ calculated from the model fields using (13). The solid line is the daily value; the dashed line is a running average over a time period of $200\sqrt{\mathrm{Ri}}/f = 93$ days. (b) Maximum value of the space and time averaged (over $200\sqrt{\mathrm{Ri}}/f$) c_e as a function of the interface displacement across the front h/H for both the two layer cases (squares) and the three layer cases (stars).

b. Equilibration of local surface cooling

A second set of high-resolution numerical calculations is now considered in which the strong frontal region results from spatial inhomogeneities in the surface buoyancy flux. These calculations complement the unforced spindown calculations from the previous section in several ways. First, the forced problems approach a statistical equilibrium in which a strong frontal region is maintained, whereas the unforced front loses considerable potential energy over the course of integration. Second, the front in the forced problems is generated by a very different mechanism than in the unforced problems. Third, the eddies that form in the forced problem have a strong barotropic component and do not look much like the two-layer hetons of the unforced problems. Finally, in the forced problems the two primary parameters, the alongfront velocity V_m and the cross-front density difference $\Delta\rho$, change in time, with their values at equilibrium being determined by the efficiency of the lateral eddy heat transport, while in the spindown configuration these parameters are set by the initial conditions. Therefore, the forced problem provides a test of the generality of the theoretical ideas presented in section 2.

The forced problems follow the shallow convection calculations described by Chapman (1998). A constant negative buoyancy flux B_0 (i.e., cooling) is applied within a circular region of radius L_0 at the surface of a resting, homogeneous ocean of depth H. The forcing abruptly vanishes outside the radius L_0. This is not terribly realistic, but it is a case that has received considerable attention and it ensures that a narrow front forms, that is, with the horizontal scale of the internal deformation radius. Initially, the dense water produced beneath the buoyancy flux mixes rapidly to the bottom, so the density anomaly increases linearly with time. A front is established around the edge of the forcing region, which begins to slump radially outward at the bottom and inward at the surface, adjusting toward geostrophy. This generates a rim current flowing around the edge of the forcing region, cyclonic at the surface and anticyclonic at the bottom. The rim current is baroclinically unstable, so waves grow rapidly into eddies that break away from the rim current and exchange dense water from beneath the imposed buoyancy flux with ambient water. Eventually a quasi equilibrium is approached in which the loss of buoyancy at the surface is balanced, in a statistical sense, by the eddy exchange across the rim current. By assuming such an equilibrated state, Visbeck et al. (1997) derived expressions for the equilibrium density anomaly within the forcing region and the time required to reach equilibrium in the shallow convection case, based on externally imposed parameters,

$$\Delta\rho_f = \left(\frac{1}{2c_e}\right)^{2/3} \frac{\rho_0}{gH}(B_0 L_0)^{2/3}; \qquad t_f = \left(\frac{1}{2c_e}\right)^{2/3} \left(\frac{L_0^2}{B_0}\right)^{1/3}, \tag{14}$$

where c_e is defined as in (2). Visbeck et al. (1997) did not actually test (14), but Chapman (1998) has shown that (14) is reasonable, at least for a few examples.[3]

Therefore, we use the same basic model configuration as Chapman (1998) to estimate c_e for several parameter combinations. The model is the semispectral primitive equation model described by Haidvogel et al. (1991). The model domain is a straight channel with periodic boundaries at the open ends. The boundaries are placed far enough from the forcing region that they have negligible influence during the model calculations. A rect-

[3] Note that Chapman (1998) used the surface velocity in his derivation of the equilibrium quantities, rather than the total vertical change in geostrophic velocity over the depth H, as used here to define V_m in (2). Consequently, Chapman's eddy exchange coefficient α is twice our efficiency constant c_e for the shallow convection case.

angular grid is used in the horizontal with either 1-km or 1.5-km resolution in each direction, depending on the parameter choices. Nine Chebyshev polynomials are used to resolve the vertical structure. A convective adjustment scheme mixes the density field whenever it is statically unstable, and small lateral Laplacian subgrid-scale mixing is used to ensure numerical stability. The model is run until the density anomaly below the center of the forcing region approaches a quasi-steady value. Further model details may be found in Chapman (1998).

The horizontal velocity together with the density anomaly at both the surface and the bottom are shown in Figs. 5a and 5b for a typical calculation as equilibration is approached. Several large eddies can be seen moving away from the forcing region (indicated by the solid circle). Their surface velocities are clearly cyclonic (Fig. 5a) with a weaker cyclonic signature at the bottom (Fig. 5b). Careful examination of the bottom velocities shows that each cyclonic eddy has an anticyclonic partner that is horizontally offset and has little, if any, signature at the surface. Cross sections of density or velocity (not shown) reveal that the eddy pairs are tilted in the vertical and overlap, somewhat like those described for the two-layer system (section 2), despite their barotropic nature. Time sequences of the velocity and density fields show that the eddy pairs indeed propagate away from the forcing region, much like the eddy pairs in the unforced problem described above. We might then expect the overall behavior to be consistent with the theoretical development in section 2.

The efficiency constant c_e can be estimated from calculations like that shown in Fig. 5, as the system approaches equilibration, by solving (14) for c_e

$$c_e = \frac{B_0 L_0}{2}\left(\frac{\rho_0}{gH}\right)^{3/2}\left(\frac{1}{\Delta\rho_f}\right)^{3/2}. \tag{15}$$

As stated above, the density anomaly beneath the buoyancy flux initially increases linearly with time. After the eddies have grown large enough to break away from the rim current (as in Fig. 5), the density anomaly oscillates about a quasi-equilibrium value, from which $\Delta\rho_f$ is estimated by averaging the surface density anomaly within a small area in the center of the forcing region. Table 1 shows estimates of c_e from (15) for five model calculations along with other model parameters. The estimates of c_e fall within the range 0.02–0.03, close to the value obtained by Visbeck et al. (1996) for deep convection and not far from the values obtained for the unforced problems in section 3a. The uncertainty in c_e represents the effects of individual eddy formation events. The values are somewhat smaller than the theoretical value of 0.045, but considering the numerous assumptions in section 2 that are not strictly applicable to these calculations, the agreement is quite good.

It is interesting to point out that eddies form prior to equilibration, but these eddies are smaller than those formed during equilibration (because of the smaller internal deformation radius), and the heat flux they carry is not sufficient to balance the surface cooling. Therefore, the density anomaly continues to increase. Because c_e is limited in magnitude by the eddy–eddy interactions, as discussed in section 2, the system can only approach equilibration when the density anomaly has increased sufficiently to form larger eddies, which propagate faster and carry more mass.

4. Summary

We have derived a quantitative means to estimate the amplitude of lateral heat transport by baroclinic eddies generated in narrow frontal zones in terms of the properties of the mean flow. The theory predicts that the eddy heat flux is linearly related to the product of the alongfront velocity scale and the cross-front density gradient as

$$\overline{u'\rho'} = c_e V_m \Delta\rho, \tag{16}$$

where c_e is an efficiency constant, $V_m = \sqrt{g'h}\sqrt{h/H}$ is the maximum alongfront velocity for a front of deformation radius width, $\Delta\rho$ is the density change across the front, h is the isopycnal displacement across the front, and H is the resting depth of the isopycnal. This expression for the eddy heat flux is similar to the form proposed by Green (1970) to parameterize eddy fluxes in the atmosphere and applied more recently to the ocean by Visbeck et al. (1996, 1997), Jones and Marshall (1997), Chapman and Gawarkiewicz (1997), and Chapman (1998).

Our approach in deriving this relationship is quite different from the energetic arguments used by Green (1970), and the scaling approach of Jones and Marshall (1997). The eddy heat flux is interpreted as the product of the average density anomaly of an eddy and its propagation speed away from the front, as given by (4). The advantage of this approach is that it eliminates the need to estimate the correlation between the eddy swirl velocity and the perturbation density (typically much less than one) as required for the traditional definition of the eddy heat flux. The problem then becomes that of determining the propagation speed of an eddy in terms of the frontal parameters where the eddy was formed. By developing the theory based explicitly on the way eddies interact and transport heat, we are able to analytically calculate the efficiency constant c_e that determines the amplitude of the cross-front heat flux, or the efficiency of the heat flux relative to the strength of the front. The efficiency constant c_e may be thought of as the ratio of the eddy propagation speed to the alongfront velocity. If it is assumed that the heat transport is carried primarily by quasigeostrophic eddy pairs of uniform potential vorticity, the efficiency constant c_e can be represented in simple integral form, which produces a theoretical estimate of $c_e = 0.045$.

This estimate was tested using three-dimensional, eddy-resolving, primitive equation models for two flow

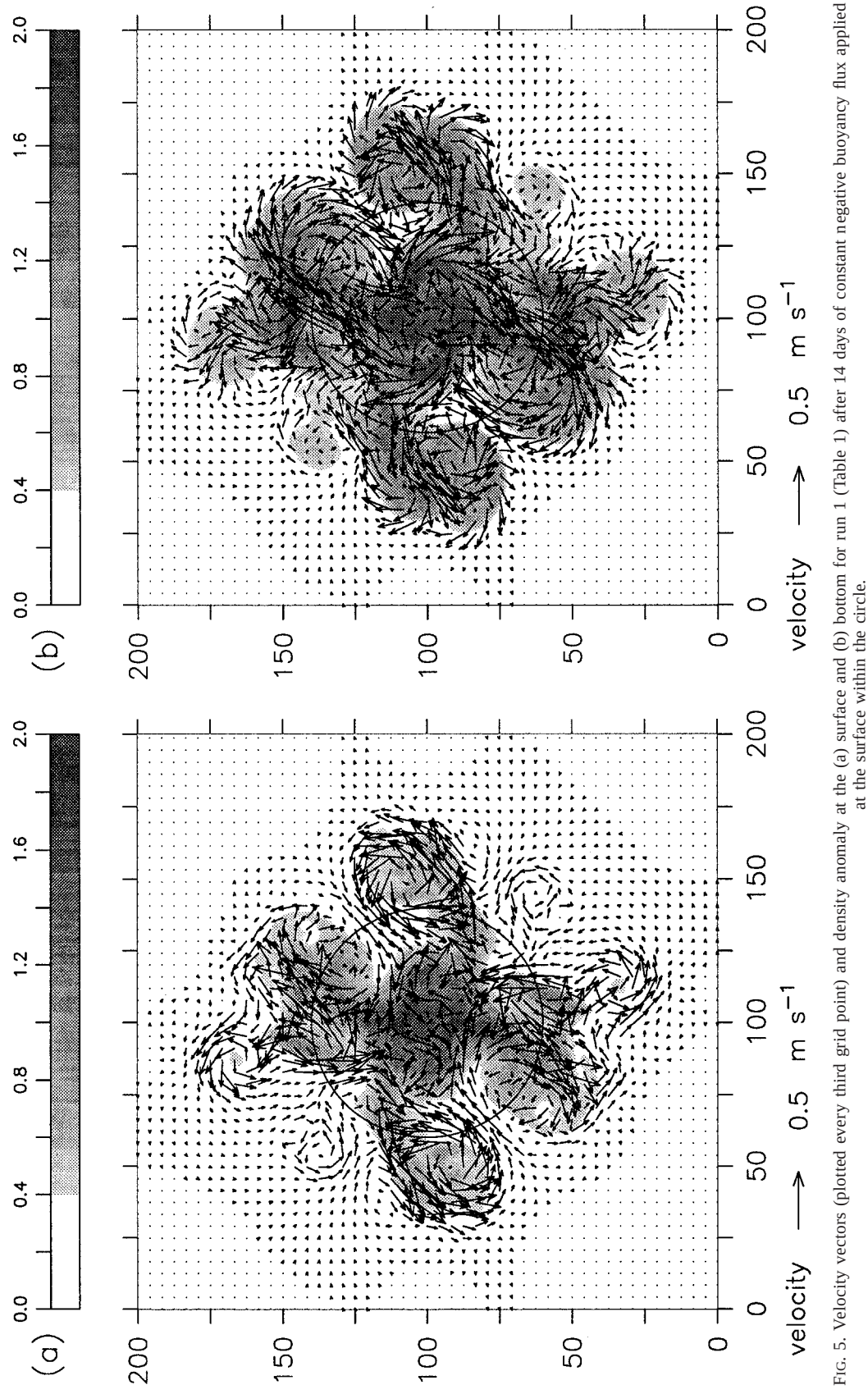

FIG. 5. Velocity vectors (plotted every third grid point) and density anomaly at the (a) surface and (b) bottom for run 1 (Table 1) after 14 days of constant negative buoyancy flux applied at the surface within the circle.

TABLE 1. Parameters and efficiency constant c_e for the forced numerical calculations discussed in section 3b. For each calculation, the initial density is $\rho_0 = 1000$ kg m^{-3}, and the depth is $H = 50$ m. Units are m^2 s^{-3} for B_0, km for r_0, s^{-1} for f, m^2 s^{-1} for the lateral viscosity ν_u.

Run	B_0 ($\times 10^{-7}$)	r_0	f ($\times 10^{-4}$)	ν_u	c_e
1	8	40	1.3	25	0.026
2	4	40	1.3	25	0.020
3	4	20	1.3	25	0.020
4	4	20	0.65	25	0.019
5	4	20	1.3	10	0.028

configurations. One set of calculations was initialized with a narrow frontal region and allowed to evolve in the absense of external forcing. The second set of calculations applied a region of surface cooling (negative buoyancy flux) over an initially motionless, homogeneous ocean, which develops a narrow front along the edge of the cooling region. In both cases, the alongfront current is baroclinically unstable, leading to lateral heat transport by baroclinic eddies. The quantitative value of c_e derived from these eddy-resolving numerical models varied between 0.02 and 0.04 over a wide range of model parameters. This compares reasonably well with the theoretical estimate of $c_e = 0.045$. The reduced efficiency in the numerical models probably arises from the finite width of the baroclinic fronts and the time it takes for meanders to reach large amplitude; both effects are neglected in the theory. Despite the quantitative differences, these results clearly support the form for the eddy heat flux in (2) and also indicate that c_e is basically independent of external parameters.

The theory was derived assuming flat-bottom, f-plane, quasigeostrophic dynamics, although the theoretical estimate is found to be reasonably accurate well beyond the formal quasigeostrophic limits. Allowing for either a sloping bottom or a variable Coriolis parameter introduces another length scale into the problem, $l = \sqrt{U/\beta}$, where β is the cross-front variation in the background vorticity. For the surface intensified, narrow frontal problems studied here, the influences of bottom topography or variations in the Coriolis parameter are negligible because the cross-front potential vorticity gradient is dominated by the change in stratification across the front. These effects may become more important for wide frontal regions, for weak stratification, or for estimating the eddy heat flux far from a narrow front. Even in these cases, however, baroclinic eddy pairs may remain a primary heat transport mechanism (with modifications due to β), although not necessarily the only one, and, if so, the general arguments presented here should remain relevant.

It has been assumed that the frontal region remains narrow and baroclinically unstable, and that the surrounding waters are not strongly populated with eddies. We recognize that steep bottom topography, planetary vorticity gradients, and large-scale confluent flows can stabilize even strong baroclinic fronts and inhibit the formation of eddies, resulting in regimes for which the present theory is not appropriate. Further, the present theory may need modification when applied to wider frontal regions because the properties of the eddies (e.g., density anomaly) will depend on their origin and mixing along their path. However, it is encouraging that Chapman (1998) found eddy heat fluxes to be only weakly dependent on the width of the baroclinic zone, so the essential mechanisms of eddy heat transport may not be strongly dependent on this length scale.

We have assumed that all eddies formed at the front propagate away from the front and never return. We have not attempted to predict their ultimate evolution and fate. That is, we do not attempt to predict the divergence of the eddy heat flux (or equivalently the eddy flux far away from the frontal region), a quantity that is perhaps of more practical interest for large-scale climate models. While the correspondence between large eddy energies and variations in the mean flow (Treguier et al. 1997) suggests that eddies decay rapidly away from their source region, the relationship between the divergence of the eddy flux and the mean flow is not clear. The present local parameterization of the eddy flux does not consider nonlocal sources, such as advection of eddy variance by the mean flow or coherent vortices generated at distant regions (such as meddies or Agulas rings).

Acknowledgments. Support for this work was provided by the Office of Naval Research (MAS, Contract N00014-97-1-0088) and the National Science Foundation as part of the Arctic System Science (ARCSS) program, which is administered through the Office of Polar Programs, (DCC, Grant OPP-9422292). Comments from two anonymous reviewers helped to clarify the discussion. Joe Pedlosky is thanked for providing comments on an early version of the manuscript.

REFERENCES

Chapman, D. C., 1998: Setting the scales of the ocean response to isolated convection. *J. Phys. Oceanogr.,* **28,** 606–620.

——, and G. Gawarkiewicz, 1997: Shallow convection and buoyancy equilibration in an idealized coastal polynya. *J. Phys. Oceanogr.,* **27,** 555–566.

Gent, P. R., and J. C. McWilliams, 1990: Isopycnal mixing in ocean circulation models. *J. Phys. Oceanogr.,* **20,** 150–155.

Green, J. S., 1970: Transfer properties of the large-scale eddies and the general circulation of the atmosphere. *Quart. J. Roy. Meteor. Soc.,* **96,** 157–185.

Haidvogel, D. B., J. L. Wilkin, and R. Young, 1991: A semi-spectral primitive equation ocean circulation model using vertical sigma coordinates and orthogonal curvilinear horizontal coordinates. *J. Comput. Phys.,* **94,** 151–185.

Hogg, N. G., and H. M. Stommel, 1985: The heton, an elementary interaction between discrete baroclinic geostrophic vortices and its implications concerning eddy heat-flow. *Proc. Roy. Soc. London,* **A397,** 1–20.

Jones, H., and J. Marshall, 1997: Restratification after deep convection. *J. Phys. Oceanogr.,* **27,** 2276–2287.

Killworth, P. D., 1983: On the motion of isolated lenses on a beta plane. *J. Phys. Oceanogr.*, **13,** 368–376.

Larichev, V. D., and I. M. Held, 1995: Eddy amplitudes and fluxes in a homogeneous model of fully developed baroclinic instability. *J. Phys. Oceanogr.,* **25,** 2285–2297.

Legg, S., H. Jones, and M. Visbeck, 1996: A heton perspective of baroclinic eddy transfer in localized open ocean convection. *J. Phys. Oceanogr.,* **26,** 2251–2266.

Pakyari, A., and J. Nycander, 1996: Steady two-layer vortices on the beta-plane. *Dyn. Atmos. Oceans,* **25,** 67–86.

Pedlosky, J., 1985: The instability of continuous heton clouds. *J. Atmos. Sci.,* **42,** 1477–1486.

Polvani, L. M., 1991: Two-layer geostrophic vortex dynamics. Part 2. Alignment and two-layer V-states. *J. Fluid Mech.,* **225,** 241–270.

Stone, P. H., 1972: A simplified radiative–dynamical model for the static stability of rotating atmospheres. *J. Atmos. Sci.,* **29,** 405–418.

Spall, M. A., 1995: Frontogenesis, subduction, and cross-front exchange at upper ocean fronts. *J. Geophys. Res.,* **100,** 2543–2557.

Treguier, A. M., I. M. Held, and V. D. Larichev, 1997: On the parameterization of quasigeostrophic eddies in primitive equation ocean models. *J. Phys. Oceanogr.,* **27,** 567–580.

Visbeck, M., J. Marshall, and H. Jones, 1996: Dynamics of isolated convective regions in the ocean. *J. Phys. Oceanogr.,* **26,** 1721–1734.

——, ——, T. Haine, and M. Spall, 1997: On the specification of eddy transfer coefficients in coarse-resolution ocean circulation models. *J. Phys. Oceanogr.,* **27,** 381–402.